An Impulse Response Model and Q factor Estimation for Vehicle Cavities

Steven Herbert, *Student Member, IEEE,* Tian Hong Loh, *Member, IEEE,* and Ian Wassell

***Abstract*—To facilitate efficient communications (i.e., minimum power consumption and maximum information throughput) in vehicle cavities, it is necessary to fully understand the underlying physics of the propagation process. This can be characterised as a statistical model of the channel impulse response, which we derive from a general starting point. The impulse response model is useful is its own right for ultra-wideband pulse radio communications, channel simulations and time of arrival positioning systems, and it also allows us to verify the generally accepted property that the energy retained in the cavity decays exponentially with time after an impulse input. This property can be characterised as a cavity Q factor, and we investigate methods of Q factor estimation in vehicle cavities, using only a limited amount of data, such as would typically be available to a deployed in-vehicle wireless network. We find that the most reliable approach utilises is an inverse discrete Fourier transform based method, which finds the maximum likelihood instantaneous Q factor, given measured data across various spatial links and frequency channels.**

***Index Terms*—Impulse response, ray tracing model, vehicle cavity, Q factor, reverberation chamber, channel sounding.**

I. Introduction

WIRELESS devices are increasingly being deployed in vehicle cavities. Infotainment systems must co-exist alongside the vehicle radio, wi-fi, mobile phones, Bluetooth headsets, and wireless sensor networks (WSNs) [1]. To deploy effective wireless systems in vehicle cavities, it is essential to understand the physics of the electromagnetic wave propagation.

The impulse response of a channel is sufficient for complete characterisation, however the vehicle cavity is fundamentally a dynamic environment (i.e., there are moving objects such as passengers within it), therefore the impulse response is itself a time varying function. For simplicity in this paper we deal only with the instantaneous impulse response (we perform our measurements in cavities unoccupied by humans or other moving objects to avoid time variation affecting our results). Previously there has been some success [2] with fitting the Saleh-Valenzuela model [3] to the impulse response of in vehicle channels, however we observe from the impulse response measurements presented in Section IV that in general the clustered structure of the Saleh-Valenzuela model may not apply to vehicle cavities. We therefore derive a theoretical model for a general case of a cavity channel, where we assume no correlation between arriving rays, in Section IV and validate it with the measurements detailed in Section II and III.

Our model is expressed in terms of five parameters which relate directly to the properties of the arriving rays. We assert that this model is directly applicable to ultra-wideband pulse radio communications, channel simulations and time of arrival positioning systems, however we also show that it is consistent with the observed exponential decay model of energy retained in vehicle cavities [4], which is also the accepted model for the reverberation chamber [5]. Such cavities can be characterised by a single parameter, its quality 'Q' factor, which is related to the time constant of the expontial decay. For narrowband communications applications, where individual rays cannot be resolved, it is more appropriate to simply characterise the channel in terms of the Q factor. Most of the existing work in this area relates to reverberation chambers, and we note that these are in general designed to be tightly controlled electromagnetic propagation environments [6], [7], and therefore Q factor estimation by a deployed in-vehicle wireless network may differ somewhat from that undertaken in a reverberation chamber. In Section V we propose three methods for Q factor estimation that can be employed by a typical narrowband wireless network, e.g., a WSN.

II. Experimental Method

We undertook two measurement campaigns. The first a broadband frequency sweep using a vector network analyser (VNA), from which we found an approximate impulse response via an inverse discrete Fourier transform (IDFT), the second a narrowband frequency sweep, which we believe is typical of the data that can be gathered by an idealised form of an in-vehicle WSN.

This work is supported by the U.K. Engineering and Physical Sciences Research Council (EPSRC) and National Physical Laboratory (NPL) under an EPSRC-NPL Industrial CASE studentship programme on the subject of Intra-Vehicular Wireless Sensor Networks. Tian Hong Loh is supported by the 2009-2012 Physical Programme of the National Measurement Office, an Executive Agency of the U.K. Department for Business, Innovation and Skills (BIS) under Project 113860.

Steven Herbert is with the Computer Laboratory, University of Cambridge, CB3 0FD, UK, and the National Physical Laboratory, TW11 0LW, UK. Contact: sjh227@cam.ac.uk

Tian Hong Loh is with the National Physical Laboratory, TW11 0LW, UK. Contact: tian.loh@npl.co.uk

Ian Wassell is with the Computer Laboratory, University of Cambridge, CB3 0FD, UK. Contact: ijw24@cam.ac.uk

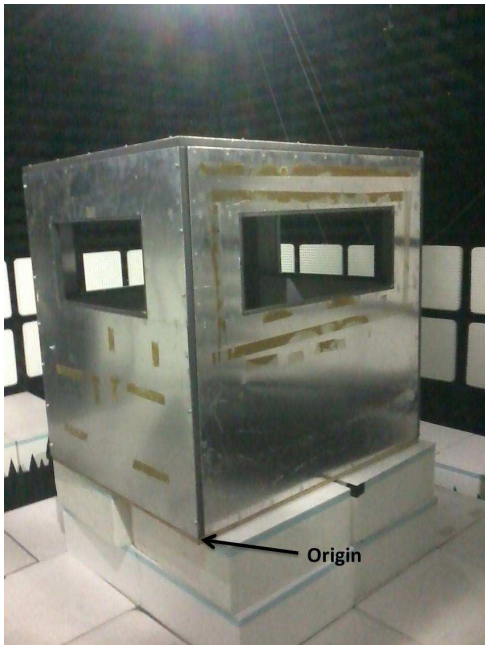

Fig. 1. The Vehicle Like Cavity.

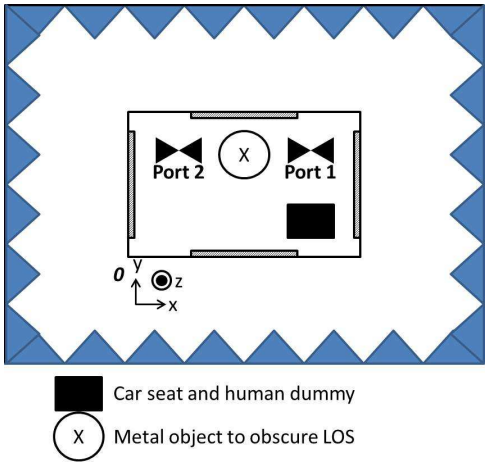

Fig. 2. The measurement set-up for the Broadband VNA Frequency sweep.

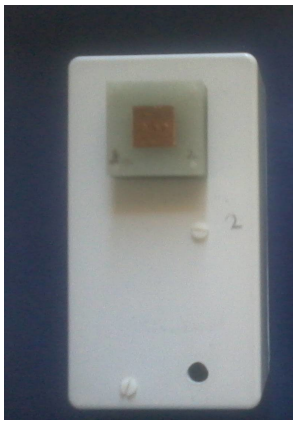

Fig. 3. WSN unit with low-profile TM_{21}^{Z} higher-order mode patch antennas.

A. Broadband Measurements

The purpose of performing a broadband frequency sweep is to subsequently undertake an IDFT to approximate the channel impulse response. The requirements of the frequency sweep are therefore that the total bandwidth must be as large as possible to achieve the greatest possible temporal resolution. The frequency resolution must be sufficient such that the total time duration of the impulse response is much greater than the time constant of exponential decay. We chose a frequency sweep of 4 - 17 GHz at a resolution of 1 MHz to satisfy these requirements, and the VNA was set to an output power of 0 dBm. The measurements were undertaken in a metal cavity known to have similar electromagnetic radiation propagation properties to those of a vehicle cavity (the cavity was the one used in the 'SEFERE' project [8]) which is shown in Figure 1. To mimic a real scenario we also added a car seat with a human dummy (i.e., having the same dielectric properties as human tissue) sitting on it. The box was located in a fully anechoic chamber, which had the advantage, compared to performing the measurements in an actual car parked outside, of a much lower noise floor. We were also able to use a VNA with a much greater frequency range than that of the portable one which we would have had to use had we performed the measurements outdoors in a real car.

The measurement set-up is shown in Figure 2. The origin ('*O*') is defined in the figure, at the floor of the cavity. The cavity has dimensions 1260 mm $\times$ 1050 mm $\times$ 1220mm (x $\times$ y $\times$ z). It has four rectangular appertures with corners located: 1) (0, 230, 700) mm, (0, 230, 1000) mm, (0, 820, 700) mm, (0, 820, 1000) mm; 2) (1260, 230, 700) mm, (1260, 230, 1000) mm, (1260, 820, 700) mm, (1260, 820, 1000) mm; 3) (230, 0, 700) mm, (230, 0, 1000) mm, (1030, 0, 700) mm, (1030, 0, 1000) mm; 4) (230, 1050, 700) mm, (230, 1050, 1000) mm, (1030, 1050, 700) mm, (1030, 1050, 1000) mm. Ports 1 and 2 of the VNA were connected to Schwartzbeck 9112 antennas, both horizontally polarised, and were located at (860, 920, 650) mm and (170, 120, 650) mm respectively. An irregular metal object was positioned to totally obscure the line of sight (LOS).

B. Narrowband Measurements

The narrowband measurements were undertaken to investigate how we can estimate the cavity Q factor using a WSN system. To simulate the WSN we positioned the WSN type units, shown in Figure 3, close to the cavity walls, where we would expect the sensors to be located in a practical deployment. Each unit consists of a box to house a wireless sensor node, and is equiped with a low-profile TM_{21}^{Z} higher-order mode patch antenna [9]. For our measurements we have dispensed with the wireless sensor nodes and used a co-axial cable to connect each pair of nodes to the VNA. We measured the channel frequency response at the sixteen *802.15.4* channels [10] (i.e., 2.405 - 2.48 GHz at a resolution of 5 MHz), and the VNA was set to an output power level of 0 dBm. Note that *802.15.4* has been chosen as it provides the physical layer for *Zigbee* [11] which in turn is used in a large

Fig. 4. Lab Car: (a) Car; (b) Unit 1 - dashboard; (c) Unit 2 - front driver side door; (d) Unit3 - rear passenger side door; (e) Unit 4 - boot driver side window;- (f) Unit 5 - boot passenger side floor.

Fig. 5. NPL Van: (a) Unit 1 - dashboard; (b) Unit 2 - middle seat headrest; (c) Unit 4 - passenger door; (d) Unit 3 - middle floor.

number of the available WSN systems, such as *Micaz* [12].

Measurements were undertaken in the unoccupied lab car where five antenna locations were used (i.e., ten links), as shown in Figure 4. In the unoccupied NPL van, four antenna locations were used (six links), as shown in Figure 5. In each case every permutation of pairs of units were connected to the VNA, in a Single-Input Single-Output (SISO) set-up.

III. Processing the Broadband Frequency Sweep to Approximate the Impulse Response

From the measured broadband frequency sweep, we estimated the channel impulse response using the following approach:

1) We note that the measured S parameters include the antennas, however using standard S matrix theory we removed their effect. We used a reverberation chamber to measure $S11$ ($S11_{meas}$) and the efficiency (η) of the antennas, and modelled each antenna as a two port S network, using the following S parameters, adapted from [13]:

$$\begin{aligned} \text{Transmitter:} \quad & S11 = S11_{meas} \\ & S21 = S12 = \sqrt{\eta}\frac{1 - S11_{meas}}{|1 - S11_{meas}|} \\ & S22 = 0 \\ \text{Receiver:} \quad & S11 = 0 \\ & S21 = S12 = \sqrt{\eta}\frac{1 - S11_{meas}}{|1 - S11_{meas}|} \\ & S22 = S11_{meas} \end{aligned}$$

2) We know that the receive antenna collects energy over an apperture with area that is inversely proportional to the frequency of operation squared. We therefore normalise across the frequency sweep by multiplying $S21$ by the frequency (i.e., as S parameters have the same dimensions as the square root of power, note that as the angle of arrival of the ray is not in general the direction of maximum gain, we do not need to scale by the gain).

3) We perform an IDFT on the normalised $S21$ measurements.

4) We make a subjective judgement regarding the point at which the impulse response becomes indistinguishable from the noise floor, and truncate the impulse response.

5) We make a subjective judgement regarding a suitable threshold above which the received power is the result of received impulses, and set all values below this to zero, leading to a discretised form of the impulse response. In this instance 5×10^{-4} was found to be a suitable threshold (i.e., see Figure 6).

6) We set all values to zero at times before t_0, i.e., the time of flight of a ray travelling along the LOS (in this case $t_0 = 3.52 \times 10^{-9} s$.

7) We square the absolute value of the response at each time instant to get the response to an impulse of energy.

8) We normalise the total energy received to unity.

Figure 6 shows the resulting impulse response. We also achieved similar results with different antenna orientations

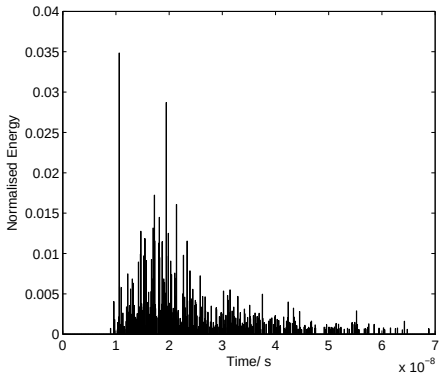

Fig. 6. Impulse Response of the Electromagnetic Cavity.

and positions of the metal object.

IV. An Impulse Response Model for Electromagnetic Cavities

From Figure 6 we observe that the impulse response does not exhibit ray arrival clustering required by the Saleh-Valenzuela model, or indeed any other apparent structure. The enclosed nature of the electromagnetic cavity means that in general we cannot assume that successive rays have taken similar paths, therefore we derive an impulse response model which does not rely on objects to give it structure, specifically we assume:

1) All rays arrive independently.

2) All rays are attenuated independently.

Strictly speaking the impulse response is a deterministic phenomenon, therefore we can formulate it statistically by noting that a cavity has some statistical properties from which we can estimate an impulse response for arbitrary transmitter and receiver locations.

We seperate the statistical impulse response into a ray arrival process and a ray attenuation process, derived in sections IV-A and IV-B respectively. In each case we start with a simple scenario and then add in complicating factors to model the real environment. In section IV-C we validate the model using our measurements.

A. Ray Arrival Process

The impulse response, $y(t)$ is derived in terms of a number of received rays (of which the i^{th} has magnitude A_i and delay τ_i, as shown):

$$y(t) = \sum_{i=1}^{\infty} A_i \delta(t - \tau_i), \tag{1}$$

where t is time, and $\delta()$ is the Dirac delta function.

We characterise the random arrival of rays in terms of their arrival time, and it is known that the Poisson process models the most general arrival process, where all rays arrive independently [14]. The number of arrivals, n, in a time interval Δt is modelled as a Poisson distribution, with probability density function (PDF):

$$P(n) = \frac{(k_b \Delta t)^n e^{-k_b \Delta t}}{n!}, \tag{2}$$

with ray arrival rate, $k_b\,[s^{-1}]$, (typically λ would be used, however k_b is used here to avoid later ambiguity with wavelength). Here and below the notation "[.]" is used to denote the units of the given parameter.

Equation 2 is the *Homogenous* Poisson process PDF, and is only valid if the parameter, k_b does not vary with time. This is not the case for our process, so we can only consider Equation 2 to be valid where the time interval, Δt, is sufficiently short such that k_b is approximately constant.

To find the variation of k_b with time, we consider a cavity which is completely closed by a perfectly reflective boundary, and consists of a constant, lossless medium. We assume the transmitter to be a point source with an isotropic radiation pattern and the receiver to also have an isotropic radiation pattern and to have a small apperture (as we are using the antenna to approximate the signal at a point). Consider a time interval Δt which is sufficiently short such that k_b is approximately constant, hence we can write an expression for the expected energy arriving in this time:

$$E(En_{tot}) = E\left(\sum_{all\,rays} En_{ray}\right), \tag{3}$$

$$= E(n) \times En_{ray}, \tag{4}$$

$$\propto k_b \Delta t \times t^{-2}, \tag{5}$$

where $E(.)$ is the expectation, En_{tot} is total energy, En_{ray} is the energy of a ray, which is deterministic and proportional to t^{-2} as the medium is constant. The expectation of a Poisson random variable is equal to its parameter, in this case $k_b \Delta t$. In a lossless medium, to obey the law of the conservation of energy, Equation 5 must not vary with t (specifically it must be proportional to Δt at any t), therefore $k_b \propto t^2$. We can therefore further define k_b:

$$k_b = k_{b0} t^2, \tag{6}$$

where $k_{b0}\,[s^{-3}]$ is a parameter.

Allowing for a Variable Medium

Consider a (theoretical) medium which is lossless, but has regions of varying propagation velocity. Our original assumption of a Poisson process is still valid, even though previously we have used the property that in a constant medium the power decay of a ray is proportional to t^{-2}. In general the decay of ray power is inversely proportional to the square of distance travelled. Consider Equation 3, where the energy of a ray is

not known deterministically. We assume that many rays arrive in the time interval Δt:

$$E(En_{tot}) = E\left(\sum_{all\ rays} En_{ray}\right), \tag{7}$$
$$\approx E(n) \times E(En_{ray}), \tag{8}$$
$$= k_b \Delta t \times E(En_{ray}), \tag{9}$$
$$\propto k_b \Delta t \times t^{-2}. \tag{10}$$

Equation 10 arrises since the mean of the decaying power is proportional to t^{-2}, and therefore the characterisation of the arrival process for a cavity filled with a variable medium is the same as that for a constant medium. In simple terms we can say that the random arrival process has absorbed the randomness of the time of flight, which means that our arrival process model generalises to the case where the rays propagate through a non-uniform medium.

Adjusting the Arrival Process for a Cavity with Appertures

Consider a cavity with appertures. Now suppose that these appertures are enclosed by an arbitrary surface to form a completely closed boundary, such as those analysed previously.

The impulse response arrival process of this cavity (i.e., with the appertures closed) can be modelled as described previously, however when the appertures are re-introduced some of the rays will be lost to the outside world. We model this as a statistical process, which for a single ray is a Bernoulli process, i.e., a ray is either lost or it is not. Let $e^{-k'_e}$ be the probability that a ray is lost, and let a given ray undergo m reflections with the cavity boundaries. We assume that each reflection with a cavity boundary is an independent and identically distributed (iid) Bernoulli random process with a probability $e^{-k''_e}$ of being lost when the appertures are reintroduced. Therefore for a ray still to exist when the appertures are reintroduced, all reflections must still exist. Therefore:

$$1 - e^{-k'_e} = 1 - \prod_{i=1}^{m} e^{-k''_e}, \tag{11}$$

$$\Rightarrow e^{-k'_e} = e^{-mk''_e}. \tag{12}$$

The number of reflections will be a random variable with the mean scaled by the time of flight, therefore we define:

$$e^{-k_e t} = e^{-mk''_e}, \tag{13}$$

where $k_e\,[s^-1]$ is a parameter.

Therefore we expect that only $e^{-k_e t}$ of the rays to remain when we re-introduce the appertures. Accordingly we must therefore scale k_b by $e^{-k_e t}$. Note that the Poisson arrival process is already a random process, so we simply scale the parameter by the mean of the ray loss process, as the randomness will be absorbed by the Poisson process. We can therefore express the general form for the distribution of the number of arrivals, n, arriving in a short time interval, Δt, at a time lapse t after an impulse as:

$$P(n) = \frac{(k_b \Delta t)^n e^{-k_b \Delta t}}{n!}, \tag{14}$$
$$k_b = k_{b0} t^2 e^{-k_e t}. \tag{15}$$

B. Ray Attenuation Process

We continue to assume that the transmitter and receiver antennas both have isotropic radiation patterns. Consider a ray to traverse a path which can be split into a large number, N, of short elements, the rays energy will be:

$$En_{ray} \propto \prod_{i=1}^{N} \left(\frac{d_i}{d_{i-1}}\right)^{-2} e^{-z_i}, \tag{16}$$

where d_i is distance to the end of the i^{th} element, and e^{-z_i} is attenuation. Note that ray power decay with distance can only be expressed in terms of ray power at some other distance, hence the distances are relative to a distance 'd_0', which is arbitrarily close to the source. An equivalent expression to 16 is:

$$En_{ray} \propto \left(\frac{d_N}{d_0}\right)^{-2} e^{-\sum_{i=1}^{N} z_i}. \tag{17}$$

We assume that the N elements are iid random variables (whilst in reality this may not be correct, in the absence of a good model for how the elements are correlated, this is the only sensible assumption we can make for the most general case, moreover as we subsequently apply the central limit theorem (CLT) it should not matter so long as the ray passes through a sufficient number of regions of the cavity). Noting that the number of elements is proportional to the ray distance, we can apply the CLT to the sum in Equation 17 to yield:

$$En_{ray} \propto \frac{d_N}{d_0} e^{-Z}, \tag{18}$$
$$Z \sim \mathcal{N}(k'_c d_N, k'_d d_N), \tag{19}$$

where $\mathcal{N}(mean, variance)$ is the normal distribution.

It is desirable to express the model as a function of time of flight, rather than distance of flight. We can do this by making the assumption that $t \propto d_N$. Note this applies if the propagation is through a constant medium, such as is typically the case in a reverberation chamber. However, in the vehicle cavity, even though the majority of the propagation is through air, there are short sections possibly through human tissue. Consequently in this case the relationship between time and distance is itself a random variable, however we choose to neglect this effect since it is expected that the attenuation incurred owing to the change of medium (such as human tissue) will dominate over the small change in the ratio of time of flight to distance. Moreover if a random variable were introduced to model the relationship between time and distance, this would not be independent of the attenuation process (since the same physical change of medium causes the attenuation and the change in ray propagation velocity),

and consequently it is non trivial to correctly model the co-dependence of these two random processes. We therefore express Equations 18 and 19 as:

$$En_{ray}{=}k_a t^{-2} e^{-Z}, \tag{20}$$

$$Z{\sim}\mathcal{N}(k_c t, k_d t), \tag{21}$$

where $k_a\,[Js^2]$, $k_c\,[s^{-1}]$ and $k_d\,[s^{-1}]$ are parameters- which is in the form of a lognormal distribution [15] scaled by $k_a t^{-2}$. We note that the ray energy in Equation 20 is also scaled by its initial energy and its receive antenna attenuation, i.e., according to the radiation patterns of the transmit and receive antennas respectively, if they are not isotropic. Depending on the specific radiation pattern, users of this model may need to introduce another random variable to account for this (i.e., as the angle from which the ray was transmitted is in general not known). We used omnidirectional antennas, which are not highly directional, and we found a good agreement with our model without needing to introduce another random variable to account for the radiation pattern.

C. Evidence for the Model

We have proposed a model for the impulse response of the vehicle cavity, with the arrival process defined in Equations 14 and 15, and the attenuation process defined in Equations 20 and 21. We now use our measurements to provide evidence which supports our model.

Arrival Process

We visualise the arrival process by plotting the inter-arrival process. It is known that a Poisson process with parameter k_b will have an exponential inter-arrival distribution, also with parameter k_b [14]. Furthermore it is known that the mean is k_b^{-1} and the variance is k_b^{-2}. We use the discretised impulse response, shown in Figure 6 to approximate the inter-arrival times of the process. This is shown in Figure 7 together with a fitted example for the mean of the inter-arrival process (i.e., as k_b is a function of time as defined in Equations 14 and 15). We observe from Figure 7 that the mean appears to be a good fit to the measured data. We also observe that as the mean value increases, so does the variation in the measured data, indeed this is to be expected, as for the exponential inter-arrival process, the mean is equal to the standard deviation.

We note that in the region approximately from 1.25×10^{-8} to 2.5×10^{-8} s, the paths are arriving so rapidly that we are probably not able to actually resolve individual rays. This conjecture is suported by the much greater energy levels observed during this time interval of the impulse response shown previously in Figure 6.

Attenuation Process

As identified in our analysis of the inter-arrival process, our discretised impulse response cannot resolve rays over its entire duration, therefore to investigate the ray attenuation process, we focus on the rays arriving at approximately 1×10^{-8} s shown in Figure 6. For simplicity we assume that the arrival time is approximately the same for all these rays, and fit

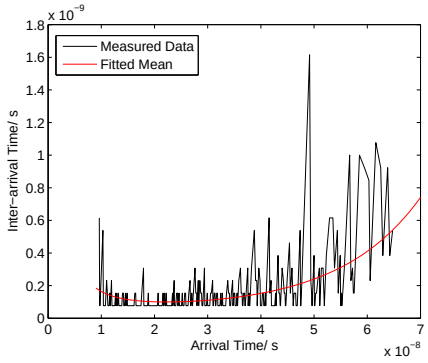

Fig. 7. Inter-arrival Times of the Process.

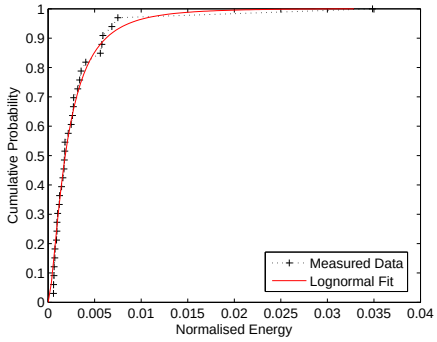

Fig. 8. Ray Attenuation Process, with Maximum Likelihood Lognormal Fit.

a lognormal distribution, shown in Figure 8. We observe a reasonably good fit, albeit with only a small number of datapoints (i.e., there were only 33 resolved rays available).

It should be noted that whilst we have provided some evidence for the lognormal distribution, we have not investigated our proposed model for the variation of the lognormal parameters with time.

Energy Retained in the Cavity

We use the expected energy in the cavity, a time t after an impulse to further support our model. We assume that in a time duration Δt a large number of paths will arrive, and the time variation of the parameters (i.e., $k_{b0} t^2 e^{-k_c t}$, $k_a t^{-}2$, $k_c t$ and $k_d t$) is small. Using the law of large numbers [16], we can say that the mean energy of the rays arriving in the time Δt equals the actual population mean. The expected energy arriving in the time interval Δt is therefore the expected number of rays, multiplied by the average energy:

$$E(En_{tot}) = E(n) \times E(En_{ray}), \tag{22}$$

where:

$$E(n){=}k_{b0} t^2 e^{-k_c t} \Delta t, \tag{23}$$

$$E(En_{ray}){=}k_a t^{-2} e^{-k_c t + \frac{k_d}{2} t}, \tag{24}$$

noting that Equation 23 arrises from the expectation of a Poisson random variable as discussed previously, and Equation 24 is the expectation of a lognormal random variable [15].

Substituting Equations 23 and 24 into Equation 22:

$$E(En_{tot}) = k_{b0} t^2 e^{-k_e t} \Delta t \times k_a t^{-2} e^{-k_c t + \frac{k_d}{2} t}, \quad (25)$$

$$= k_a k_{b0} e^{-(k_c - \frac{k_d}{2} + k_e) t} \Delta t, \quad (26)$$

$$= k e^{\frac{-t}{\tau}} \Delta t, \quad (27)$$

where we define $k = k_a k_{b0}$ and $\tau = \frac{1}{k_c - \frac{k_d}{2} + k_e}$, then dividing by Δt to get the expected power (Pow_{tot}):

$$E(Pow_{tot}) = k e^{\frac{-t}{\tau}}. \quad (28)$$

It is easiest to visualise this property by considering the expected cumulative energy (En_{cum}), which can be found by intergrating the expected power with respect to time:

$$E(En_{cum}) = \int_{t_{0'}}^{t} k e^{\frac{-t}{\tau}} \, dt, \quad (29)$$

$$= k\tau \left(e^{\frac{-t_{0'}}{\tau}} - e^{\frac{-t}{\tau}} \right). \quad (30)$$

Figure 9 shows our measurements together with a fit for the mean cumulative energy, note that we use the fact that we now know the time of arrival of the first ray, $t_{0'}$. We observe a good fit, which provides strong evidence that our impulse response is valid. In particular this justifies our scaling of the lognormal parameters k_d and k_e by the time of flight, as the expectation of this creates the exponentially decaying expectation of the total energy. An accepted property of the reverberation chamber is that the energy retained decays exponentially with time after an impulse [5] and this has also been observed to be the case in vehicle cavities [4]. We observe that our theory and measurements are consistent with this property, and this provides strong evidence for the validity of our model.

In reverberation chambers, the time constant, τ (i.e., of decay of energy) can be used to find the quality 'Q' factor of the cavity [5]:

$$Q = 2\pi f \tau, \quad (31)$$

where f is the frequency of operation.

This can also be applied to the vehicle cavity if the value of τ is the same for all possible antenna locations (i.e., as the Q factor is a property of the cavity, it therefore ceases to have a meaning if it varies with antenna location). In Section V we address the estimation of the Q factor of vehicle cavities.

V. Evaluating the Q factor of Vehicle Cavities

Preliminary measurements indicate that it is valid to analyse both the unoccupied lab car and unoccupied NPL van as cavities with a Q factor (i.e., τ is approximately the same for a variety of antenna locations). We investigate methods to use WSN systems to estimate the Q factor, in Section V-A we identify potential problems, in Section V-B we propose three methods to estimate the Q factor and in Section V-C we present the results of the Q factor evaluated according to these three methods, and discuss the relative merits of the methods.

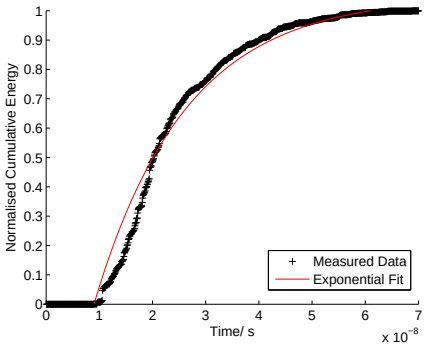

Fig. 9. Cumulative Energy with Minimum Mean Squared Error Exponential Fit.

A. Problems with Q factor Calculation in the Vehicle Cavity

Typically Q factor evaluations in a reverberation chamber are undertaken by finding the average power transferred over a large number of stirrer positions, for an arbitrary non LOS (NLOS) channel. This method makes four assumptions that are not valid in the vehicle cavity.

1) Deterministic field can be neglected: The reverberation chamber can be thought of as the addition of two electric fields, the stirred field and the deterministic field [5]. In a well designed chamber the stirred field will dominate and the deterministic field can be neglected. The analogy in the vehicle cavity is the motion of the occupants as being equivalent to stirrers, therefore it is necessary to make some further assumptions about the motion of occupants before exploiting this property to estimate the Q factor. It is therefore preferable to estimate an *instantaneous Q factor* (that is to say the power received from rays existing instantaneously and not making any assumptions concerning their existence or lack of at any other time instant) from the variation of received signal in frequency and across different channels in space.

2) Significance of LOS: It is specified that a LOS must not exist between the transmitter and receiver when evaluating the Q factor of a reverberation chamber [5]. This is because typically highly directional antennas, such as horns, are used to perform a sweep across a large frequency range. In the vehicle cavity it is envisaged that it will not be possible to exploit the LOS between two units, even if it exists in the empty cavity, as there is no guarantee that it will exist when the vehicle is loaded with occupants. The antenna is therefore designed to radiate into the cavity as uniformally as possible (i.e., it has an omnidirectional pattern) in order to exploit the reverberative environment to transfer information. In this instance if a LOS component exists it will merely be the first ray of the impulse response.

It is of course possible to place two antennas arbitrarily close together, such that the LOS path dominates to such an extent that it cannot be thought of as part of the arrival rate process, however in the first instance we shall not consider

such a scenario.

3) The Volume of the Cavity is not Clearly Defined: In the reverberation chamber, the Q factor is evaluated by the following equation [5]:

$$Q = \frac{16\pi^2 V}{\eta_{tx}\eta_{rx}\lambda^3}\langle\frac{P_r}{P_t}\rangle, \tag{32}$$

where V is the cavity volume, η is the antenna efficiency, λ is the wavelength, and P_t is the power transmitted and P_r is the power received. $\langle . \rangle$ denotes an average. This is derived by considering the energy stored per unit volume to be uniform in the reverberation chamber, however the vehicle cavity contains absorbing objects, and has large apertures, therefore the uniformity assumption is not valid- and it is therefore not possible to define the cavity volume.

4) The cavity time constant is much greater than the time of flight of a ray travelling directly between any pair of nodes: In order to apply Equation 32, not only must the cavity volume be defined, but the average power ratio $\langle\frac{P_r}{P_t}\rangle$ must be the same for all links (as we perform the average over all links). The expected ratio of power received to power transmitted of a given link can be found from Equation 29, noting that as we are now working with a constant carrier frequency input rather than an impulse, the expression is now valid as a function of power not energy:

$$\langle\frac{P_r}{P_t}\rangle = \int_{t_0}^{\infty} k e^{\frac{-t}{\tau}} \mathrm{d}t, \tag{33}$$

$$= k\tau e^{\frac{-t_0}{\tau}}, \tag{34}$$

where t_0 is arrival time of the first ray, which we approximate as the time of flight of the LOS path (i.e., this is the instant at which impulses can begin to arrive).

If $t_0 << \tau$ for all channels then $e^{\frac{-t_0}{\tau}} \approx 1$ and therefore $\langle\frac{P_r}{P_t}\rangle \approx k\tau$. If this were the case, along with having a well defined volume, then we could confidently apply Equation 32 to evaluate the Q factor, however as we have so stated this is not necessarily the case for vehicle channels.

B. Evaluation of the Q Factor of a Vehicle Cavity

As detailed in the experimental method (i.e., Section II), we aim to estimate the cavity Q factor for a practical arrangement of an in-vehicle WSN, using just narrowband measurements (i.e., as would typically be available to an in-vehicle WSN). In our case we use a VNA, however for the first two Q factor estimation methods, we use only the magnitude of the received power (i.e., analagous to the received signal strength indicator (RSSI), which is available on virtually all wireless sensor motes).

1) Q Factor Evaluation Method 1- Power Average Across Frequency and Space: Notwithstanding the issues raised in section V-A, we consider it a sensible reference to evaluate the Q factor according to Equation 32. We average over all instantaneous values of power in space (i.e., the various links) and frequency, and we use the internal volume of the car cavity as the volume.

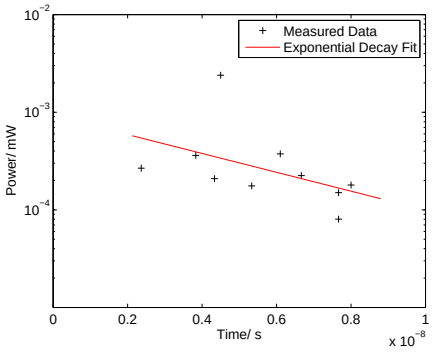

Fig. 10. Average Power Received against Time of Flight of Direct Line, for 10 links in the Lab Car, with MMSE line of best fit.

This Q factor evaluation method is defined for use in reverberation chambers, however the average will typically take place over 200 or more stirrer positions. We perform preliminary work in the reverberation chamber and achieve consistent values of Q by performing an average over 16 frequency channels at 6 spatial locations (as will be the case in the NPL van, which is the worst case scenario since we have 10 spatial positions available in the lab car) compared with the conventional Q factor evaluation that employs over 200 stirrer positions.

2) Q Factor Evaluation Method 2- Decay of Power with LOS Distance: Re-expressing Equation 34 in logarithmic form yields:

$$ln(\langle P_r\rangle) - ln(P_t) = ln(k\tau) - \frac{t_0}{\tau}, \tag{35}$$

where ln is the natural logarithm. Now if we set the transmission power to be constant and equal for all links, we can see that as $ln(P_t)$ and $ln(k\tau)$ are constants, τ (and hence the Q factor) can be estimated from the gradient of the graph of $ln(\langle P_r\rangle)$ versus t_0. This is shown for the lab car results in Figure 10.

The advantages of this method, compared to method 1 are that we do not assume that $t_0 << \tau$, and we do not require use of the cavity volume. The disadvantage is that this method relies on there being sufficient variation in link LOS distances to find the gradient, and this may not always be the case in deployed networks (and indeed when we tried this method on data gathered in the NPL van, we found that the link lengths were too similar to get meaningful results).

3) Q Factor Evaluation Method 3- Maximum Likelihood Parameter Estimation: The previous heuristic Q factor estimation methods provide an intuitive starting point for characterising the intra-vehicular radio propagation environment, however by being a little more specific about the statistical processes occuring, it is possible to find a method which uses the available information to find a Q

factor estimate that is in some sense optimal. To do this we take a Bayesian starting point, noting that our physical model means that the Q factor is the only parameter required to characterise the cavity.

Let **r** be a vector of the received power across all frequencies and channels in space, at a given time instant:

$$maximise\ P(Q|\mathbf{r}) = \frac{P(\mathbf{r}|Q)P(Q)}{P(\mathbf{r})}. \quad (36)$$

As we have no prior belief regarding the Q factor, we choose a uniform prior $P(Q)$, therefore maximum a posteriori estimation is identical to maximum likelihood estimation,

$$maximise\ P(Q|\mathbf{r}) = P(\mathbf{r}|Q). \quad (37)$$

The vector of observations **r** is a vector of Rayleigh random variables, however it is known that the frequency points at which **r** is evaluated are not independent [17]. It is not trivial to see how the statistical propagation model allows us to estimate the joint likelihood of the observation **r** in the frequency domain, however we propose that by taking an IDFT of the observations, and thus working in the time domain, it is possible to estimate this joint distribution (i.e., instead of transforming our statistical model into the frequency domain, we transform our observations into the time domain). It should be noted that for any vector of observations at a set of frequency points, there exists a dual form in the time domain. For simplicity we will look exclusively at cases with 16 equally spaced points in frequency (i.e., with a spacing between points of 5MHz). Finally, it is important to note that as the IDFT is merely a deterministic operation on the observation vector, the maximum likelihood estimate (and likelihood value) will be the same as that which would be obtained if it were possible to estimate directly in the frequency domain, provided the statistical model is applied properly.

Let $\mathbf{r}_{f,link}$ be the vector representing the observations at points in frequency, for the link in space $link$, and $\mathbf{r}_{t,link}$ be its IDFT. Now since channels in space are independent:

$$P(\mathbf{r}|Q) = \prod_{all\ links} P(\mathbf{r}_{f,link}|Q) = \prod_{all\ links} P(\mathbf{r}_{t,link}|Q). \quad (38)$$

Let n be the number of elements in the vector $\mathbf{r}_{f,link}$, therefore its IDFT, $\mathbf{r}_{t,link}$, will also be an n point vector. The resolution of $\mathbf{r}_{f,link}$ is 5 MHz, with a total frequency range of 80 MHz. This leads to a resolution in time of 12.5 ns for a maximum duration of 200ns for $\mathbf{r}_{t,link}$.

The time response $\mathbf{r}_{t,link}$ therefore takes the form of 'bins', where each element is the complex sum of all rays arriving in the corresponding time interval, which shall be noted t_- and t_+ for the lower and upper limits respectively of the i^{th} bin. Translating the time domain response to zero, and noting that this means that the first bin is centred on zero, the vector t_- and t_+ can be expressed:

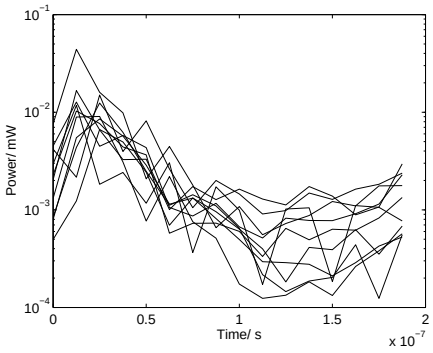

Fig. 11. IDFT of 16 Frequency Points for Lab Car- For 10 Links.

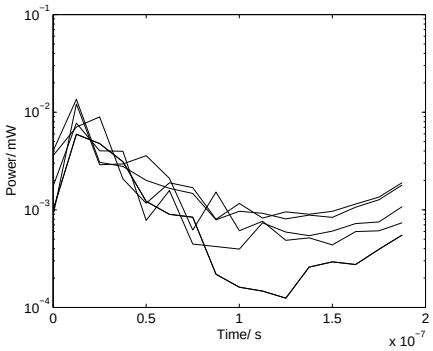

Fig. 12. IDFT of 16 Frequency Points for NPL van- For 6 Links.

$$t_-=(0; 6.25; 18.75; 31.25; 43.75; 56.25; 68.75; 81.25; 93.75; 106.25; 118.75; 131.25; 143.75; 156.25; 168.75; 181.25)\ ns, \quad (39)$$

$$t_+=(6.25; 18.75; 31.25; 43.75; 56.25; 68.75; 81.25; 93.75; 106.25; 118.75; 131.25; 143.75; 156.25; 168.75; 181.25; 193.75)\ ns. \quad (40)$$

It is noted that the contents of each bin corresponds to an independent Rayleigh random variable, where the parameter of the distribution can be found from the energy arriving during the time interval. It should be noted that the first ray will not arrive during the first bin if the LOS time $t_0 > t_+(0)$, consequently from Equation 38 we can write:

$$P(\mathbf{r}_{t,link}|Q) = \prod_{all\ n|t_0<t_+(n)} Ray(\mathbf{r}_{t,link}(n), \sigma(n)), \quad (41)$$

where $Ray(x, \sigma)$ is the Rayleigh PDF of observation x, with parameter σ - relating to the expected power in each time interval Ω:

TABLE I
Q FACTOR ESTIMATION.

	Method 1 Q	**Method 2** Q	**Method 3** Q
Lab Car	117	69	180
NPL Van	56	n/a	206

$$\Omega = \int_{max(t_-;t_0)}^{t_+} k e^{\frac{-t}{\tau}}\, dt, \tag{42}$$

$$\sigma = \sqrt{\frac{\Omega}{2}}. \tag{43}$$

This approach can best be visualised by observing that the decay of each channel in space is identical, once the first ray has arrived. This is shown in Figure 11 and Figure 12 for the lab car and the NPL van respectively. It should also be noted that after approximately 80 ns the signal reaches the noise floor, and therefore an additive white Gaussian noise (AWGN) term is included in the Q factor estimate. Note the apparent rise at the end of the plot is an artefact of the IDFT, and that the IDFT processing distorts the values of absolute power (shown on the y axis). However since our concern is with the shape of the curve, not its absolute value, this effect can be neglected.

C. Results and Discussion

The Q factor has been estimated using the three proposed methods, giving the results summarised in Table I. Heddebaut et al [18] measure the in-vehicle Q factor in the frequency range 1 - 6GHz and obtain results in the range 100 - 1000. They define the in-vehicle Q factor as the maximum observed ratio of $\frac{16\pi^2 V}{\lambda^3}\frac{|S21|^2}{1-|S11|^2}$, and therefore as expected their Q factor is typically higher than our value- but nontheless has the same order of magnitude. Ruddle [19] also estimates in vehicle Q factors in the range 100 - 1000 by performing numerical simulations.

It is encouraging to note that the values of Q factor from method 3 are consistent with previous work. The value of Q factor from method 2 is somewhat lower, probably as a result of this method using only a small amount of the total data, i.e., the difference in power received for the various links as a function of the difference in lengths of these links. Our experimental results suggest that a system designer must pay attention to the physical environment and wireless link placements (i.e., specifically a variety of separation distances) if method 2 is to yield reliable Q factor estimates. Method 1 gives values of Q which are significantly lower than those from method 3 (especially for the NPL van), which is likely to be a result of the rapid energy loss as identified in Section V-A. Nonetheless if a wireless system designer can live with this drawback then method 1 may be sufficient.

Overall however, if magnitude and phase information are available we believe that method 3 is the best approach to aggregate the available information and so yields reliable estimates of the cavity Q factor. It uses all of the available channel state information and does not require knowledge about the cavity volume and approximations concerning variable energy loss between links. It is interesting and encouraging to note, that using a small number of datapoints such as one may have available when implementing a WSN, we arrive at the same conclusion as that reached by VanT Hof [20] when conducting measurements in a reverberation chamber using many more datapoints over a much broader frequency range.

VI. CONCLUSION

We have used ray tracing analysis to propose a statistical impulse response model for the electromagnetic cavity. The model is for the general case where all rays arrive independently and are attenuated independently. We have performed measurements which provide evidence to support our model, and importantly we have shown that our model is consistent with the accepted electromagnetic cavity property that energy retained after an impulse decays exponentially with time.

For a reverberation chamber this exponential decay is parameterised by the Q factor. By carefully identifying the differences between reverberation chambers and vehicle cavities, we have shown that a reverberation chamber type analysis can also be applied to vehicle cavities. We have demonstrated successful parameter estimation (i.e., of the Q factor) using a small number of channel frequency response datapoints across a narrow band, such as would typically be available to a deployed WSN. We propose that estimating the Q factor from the decay time constant (which is found by an IDFT of the frequency response) is the best method for a wireless network deployed in a vehicle cavity.

ACKNOWLEDGMENT

The authors would like to thank Jonathan Rigelsford for the loan of the SEFERE project vehicle like cavity, and for his input with performing the measurements in it.

REFERENCES

[1] J. Dawson, D. Hope, M. Panitz, and C. Christopoulos, "Wireless networks in vehicles," in *Electromagnetic Propagation in Structures and Buildings, 2008 IET Seminar on*, dec. 2008, pp. 1 –6.

[2] N. Zhang, X. Zhu, L. Liu, C. Yu, Y. Zhang, Y. Dong, H. Zhang, Z. Kuai, and W. Hong, "Measurement and characterization of wideband channel for in-vehicle environment," in *Radio and Wireless Symposium, 2009. RWS '09. IEEE*, jan. 2009, pp. 191 –194.

[3] A. Saleh and R. Valenzuela, "A statistical model for indoor multipath propagation," *Selected Areas in Communications, IEEE Journal on*, vol. 5, no. 2, pp. 128 –137, february 1987.

[4] J. Andersen, K. L. Chee, M. Jacob, G. Pedersen, and T. Kurner, "Reverberation and absorption in an aircraft cabin with the impact of passengers," *Antennas and Propagation, IEEE Transactions on*, vol. 60, no. 5, pp. 2472 –2480, may 2012.

[5] D. Hill, *Electromagnetic Fields in Cavities(Deterministic and Statistical Theories)*, 2009.

[6] C. Bruns and R. Vahldieck, "A closer look at reverberation chambers - 3-d simulation and experimental verification," *Electromagnetic Compatibility, IEEE Transactions on*, vol. 47, no. 3, pp. 612 – 626, aug. 2005.

[7] L. Arnaut, "Statistics of the quality factor of a rectangular reverberation chamber," *Electromagnetic Compatibility, IEEE Transactions on*, vol. 45, no. 1, pp. 61 – 76, feb 2003.

[8] H. Zhang, L. Low, J. Rigelsford, and R. Langley, "Field distributions within a rectangular cavity with vehicle-like features," *Science, Measurement Technology, IET*, vol. 2, no. 6, pp. 474 –484, november 2008.

[9] C. Delaveaud, P. Leveque, and B. Jecko, "New kind of microstrip antenna: the monopolar wire-patch antenna," *Electronics Letters*, vol. 30, no. 1, pp. 1 –2, jan 1994.

[10] [Online]. Available: http://standards.ieee.org/getieee802/download/802.15.4d-2009.pdf

[11] [Online]. Available: http://www.zigbee.org/

[12] [Online]. Available: http://www.memsic.com/wireless-sensor-networks/

[13] N. R. G. Z. Prakoso, T. and T. A. Rahman, "Antenna representation in two-port network scattering parameter." *Microwave and Optical Technology Letters*, vol. 53, no. 6, pp. 1404–1409, 2011. [Online]. Available: http://dx.doi.org/10.1002/mop.26005

[14] A. Renyi, "Remarks on the Poisson process." [Online]. Available: http://www3.nd.edu/∼mhaenggi/ee87021/Renyi-RemarksPPP.pdf

[15] J. Aitchison and J. Brown, *The Lognormal Distribution*. Cambridge University Press, 1957.

[16] [Online]. Available: http://mathworld.wolfram.com/LawofLargeNumbers.html

[17] R. Liu, S. Herbert, T.-H. Loh, and I. Wassel, "A study on frequency diversity for intra-vehicular wireless sensor networks (wsns)," September 2011.

[18] M. Heddebaut, V. Deniau, and K. Adouane, "In-vehicle wlan radio-frequency communication characterization," *Intelligent Transportation Systems, IEEE Transactions on*, vol. 5, no. 2, pp. 114 – 121, june 2004.

[19] A. Ruddle, "Validation of simple estimates for average field strengths in complex cavities against detailed results obtained from a 3d numerical model of a car," *Science, Measurement Technology, IET*, vol. 2, no. 6, pp. 455 –466, november 2008.

[20] J. P. Van't Hof, "Modeling the dispersion and gain of rf wireless channels inside reverberant enclosures," Ph.D. dissertation, Dept. of Electrical and Computer Engineering, Carnegie Mellon Univ., Pittsburgh, PA, 2005.

Steven Herbert graduated in 2010 from the Signal Processing Group, Department of Engineering, University of Cambridge with a BA (subsequently promoted to MA Cantab. in 2013) and MEng degree. He is currently reading for a PhD in the Digital Technologies Group, Computer Laboratory, University of Cambridge, and the Electromagnetic Technologies Group, National Physical Laboratory.

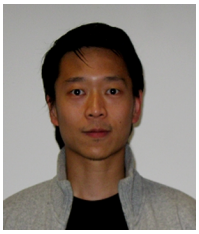

Tian Hong Loh (S'03-M'05) was born in Johor, Malaysia. He received the B.Eng. degree (first class) from Nottingham Trent University, Nottingham, U.K., and the Ph.D. degree from the University of Warwick, Coventry, U.K., in 1999 and 2005, respectively, both in electrical and electronic engineering. He joined the National Physical Laboratory, Teddington, U.K., in 2005 as a Higher Research Scientist and since 2009 he has been a Senior Research Scientist, involved in work on fundamental research and develop measurement technologies in support of the electronics and communication industry. Since 2011, he has been appointed as RF and Microwave technical theme leader, involved in physical programme formulation and strategy development. His current research interests include metamaterials, computational electromagnetics, small antenna, smart antennas, and wireless sensor networks.

Ian Wassell received his B.Sc. and B.Eng. degrees from the University of Loughborough in 1983, and his Ph.D. degree from the University of Southampton in 1990. He is a Senior Lecturer at the University of Cambridge Computer Laboratory and has in excess of 15 years experience in the simulation and design of radio communication systems gained via a number of positions in industry and higher education. He has published more than 170 papers concerning wireless communication systems and his current research interests include: fixed wireless access, sensor networks, cooperative networks, propagation modelling, compressive sensing and cognitive radio. He is a member of the IET and a Chartered Engineer.